

Anthony C. Withers · Eric J. Essene · Youxue Zhang

## Rutile/TiO<sub>2</sub>II phase equilibria

Received: 3 September 2002 / Accepted: 17 December 2002 / Published online: 6 March 2003  
© Springer-Verlag 2003

**Abstract** The transition between rutile and  $\alpha$ -PbO<sub>2</sub> structured TiO<sub>2</sub> (TiO<sub>2</sub>II) has been investigated at 700–1,200 °C and 4.2–9.6 GPa. Hydrothermal phase equilibrium experiments were performed in the multi-anvil apparatus to bracket the phase boundary at 700, 1,000, and 1,200 °C. The equilibrium phase boundary is described by the equation:  $P$  (GPa) =  $1.29 + 0.0065 T$  (°C). In addition, growth of TiO<sub>2</sub>II was observed in experiments at 500 and 600 °C, although growth of rutile was too slow to bracket unambiguously the equilibrium boundary at these temperatures. Water was not detected in either rutile or TiO<sub>2</sub>II, and dry synthesis experiments at 1,200 °C were consistent with the phase boundary determined in the fluid-bearing experiments, suggesting that the equilibrium is unaffected by the presence of water. Our bracket of the phase boundary at 700 °C is consistent with the reversed, dry experiments of Akaogi et al. (1992) and the reversals of Olsen et al. (1999). The new data suggest that the phase boundary is linear, in agreement with Akaogi et al. (1992), but in striking contrast to the phase diagram inferred by Olsen et al. (1999). The natural occurrence of TiO<sub>2</sub>II requires formation pressures considerably higher than the graphite–diamond phase boundary.

### Introduction

With increasing pressure, TiO<sub>2</sub> forms a series of post-rutile polymorphs that have increasingly dense structures, corresponding to columbite ( $\alpha$ -PbO<sub>2</sub> structure, or TiO<sub>2</sub>II, Bendeliany et al. 1966), baddeleyite ( $\alpha$ -ZrO<sub>2</sub> structure, Sato et al. 1991), and cotunnite (PbCl<sub>2</sub> structure, Dubrovinsky et al. 2001). The phase relations of these polymorphs are of interest to geologists because rutile is an important accessory mineral in metamorphic rocks including eclogites, and because they may serve as useful, lower pressure analogues for post-stishovite phases of SiO<sub>2</sub>. Moreover, to understand the significance of the recent discoveries of TiO<sub>2</sub>II and baddeleyite-structured TiO<sub>2</sub> in shocked gneiss of the Reis crater (El Goresy et al. 2001a, 2001b), and of a nanometer-thick lamella of TiO<sub>2</sub>II in a rutile inclusion in garnet from high pressure rocks of the Saxonian Erzgebirge (Hwang et al. 2000), it is necessary to investigate TiO<sub>2</sub> phase relations.

There has been considerable dispute over the equilibrium phase boundary between rutile and TiO<sub>2</sub>II. Dachille et al. (1968) used an opposed anvil apparatus to synthesize rutile and TiO<sub>2</sub>II under hydrothermal conditions, at 1–10 GPa. The phase diagram proposed by Dachille et al. (1968) was criticized by Jamieson and Olinger (1969), who noted that Dachille et al. (1968) used anatase and brookite starting materials rather than rutile. Calculation of the anatase–rutile equilibrium from thermodynamic data do not yield a stability field for anatase at or above STP, indicating that both the slope and locus of phase equilibria for TiO<sub>2</sub> by Dachille et al. (1968) are incorrect (Hayob et al. 1993). The failure of anatase to react below 500 °C is likely to be a kinetic effect resulting from the very slow reaction of anatase to form rutile.

Akaogi et al. (1992) used a cubic anvil apparatus to measure growth of rutile and TiO<sub>2</sub>II in situ. They found that reaction was sluggish below 800 °C, but by using starting material prepared in shock experiments they

---

A.C. Withers (✉) · E.J. Essene · Y. Zhang  
Department of Geological Sciences,  
University of Michigan, Ann Arbor,  
MI 48109-1063, USA  
E-mail: anthony.c.withers-1@umich.edu  
Tel.: +1-612-6243336  
Fax: +1-612-6253819

*Present address:* A.C. Withers  
Department of Geology and Geophysics,  
University of Minnesota, Minneapolis,  
MN 55455, USA

Editorial responsibility: T.L. Grove

were nonetheless able to bracket the reaction boundary at 600–900 °C. Olsen et al. (1999) also used a cubic anvil apparatus to make in situ observations of rutile and TiO<sub>2</sub>II growth. They used rutile starting material, increased temperature (starting from 25 °C) at a given high pressure, and monitored phase changes at hundred degree increments using in situ X-ray diffraction. At 5.3 GPa, where TiO<sub>2</sub>II is expected to be stable at <470 °C and rutile is expected to be stable above 470 °C according to Akaogi et al. (1992), Olsen et al. (1999) did not observe formation of TiO<sub>2</sub>II as rutile powder was heated from 25 to 1,200 °C. Clearly, the failure to observe formation of TiO<sub>2</sub>II at temperatures of 25 to 470 °C is attributable to sluggishness of the reaction from rutile to TiO<sub>2</sub>II. At 6.8 GPa, where TiO<sub>2</sub>II is expected to be stable at ≤ 870 °C (Akaogi et al. 1992), Olsen et al. (1999) observed the transition of rutile to TiO<sub>2</sub>II at 700 °C, and then back to rutile at 1,100 °C. At 7.5 GPa, where TiO<sub>2</sub>II is expected to be stable at ≤ 1,050 °C (Akaogi et al. 1992), Olsen et al. (1999) observed the transition of rutile to TiO<sub>2</sub>II at 600 °C, and then back to rutile at 1,100 °C. Although Olsen et al. (1999) recognized that the transition from rutile to TiO<sub>2</sub>II is sluggish at temperatures below 800 °C and although their data differ from those of Akaogi et al. (1992), they did not carry out reversal experiments, did not consider the possibility of a kinetic effect on the experimental results, interpreted their data to represent the true equilibrium phase boundary between rutile and TiO<sub>2</sub>II, and inferred a curved phase boundary between rutile and TiO<sub>2</sub>II. The results of Olsen et al. (1999) have been used to infer the pressure and temperature conditions for ultrahigh-pressure metamorphism (UHPM) of diamondiferous gneisses (Hwang et al. 2000; Shen et al. 2001).

With the recent discovery of naturally occurring TiO<sub>2</sub>II (Hwang et al. 2000; El Goresy et al. 2001a, 2001b), accurate knowledge of the phase boundary between rutile and TiO<sub>2</sub>II is essential for using the rutile to TiO<sub>2</sub>II phase transition to further constrain the UHPM pressure. In this study we aim to resolve the disagreement between Akaogi et al. (1992) and Olsen et al. (1999) by performing reversed, phase equilibrium experiments to determine the phase boundary between rutile and TiO<sub>2</sub>II.

## Experimental methods

High pressure experiments were carried out in the multi anvil apparatus at the University of Michigan. The multi anvil consists of a Walker style module mounted in a 1,000 ton hydraulic press (Walker et al. 1990). Tungsten carbide (Federal Carbide FC-3M) anvils with 12 mm truncated edge lengths were used with a castable MgO–SiO<sub>2</sub>–Al<sub>2</sub>O<sub>3</sub>–Cr<sub>2</sub>O<sub>3</sub> octahedral pressure medium (Aremco Ceramacast 584-OS + 2.5 wt% Cr<sub>2</sub>O<sub>3</sub>). The force-pressure relationship was calibrated at room temperature using electronic phase transitions in Bi

(Piermarini and Block 1975), and at 1,200 °C by bracketing the quartz–coesite, CaGeO<sub>3</sub> garnet–perovskite and coesite–stishovite phase transitions (Susaki et al. 1985; Zhang et al. 1993; Bose and Ganguly 1995). The room temperature calibration curve has a greater efficiency relative to the 1,200 °C calibration at the lower end (2–5 GPa) of the pressure range for the assembly (Fig. 1).

Rutile was synthesized from reagent grade anatase by heating at 1,200 °C for 24 h in a controlled atmosphere furnace. A constant flow of air was maintained over the sample to inhibit reduction to form a Ti<sub>2</sub>O<sub>3</sub> component. An earlier attempt to synthesize rutile in a muffle furnace without a constant through-flow of air resulted in the presence of reduced Ti in the sample, as indicated by blue coloring. The TiO<sub>2</sub>II phase was synthesized from anatase in the multi anvil at 9.5 GPa and a nominal temperature of 900 °C for 4.5 h under anhydrous conditions. Additional anhydrous syntheses were conducted at 1,200 °C. In these experiments, anatase was loaded directly into the rhenium furnace, and the type D thermocouple junction was located in the center of the assembly, in contact with the sample.

The starting material for the phase equilibrium experiments was an equimolar mix of rutile and TiO<sub>2</sub>II. For each experiment, the starting material, together with ~5 wt% water, was sealed in a 2-mm diameter Pt capsule, which was located in the center of the pressure cell. Temperature was measured and controlled by means of a type D thermocouple, the junction of which was in contact with the 0.3-mm thick, welded lid of the capsule.

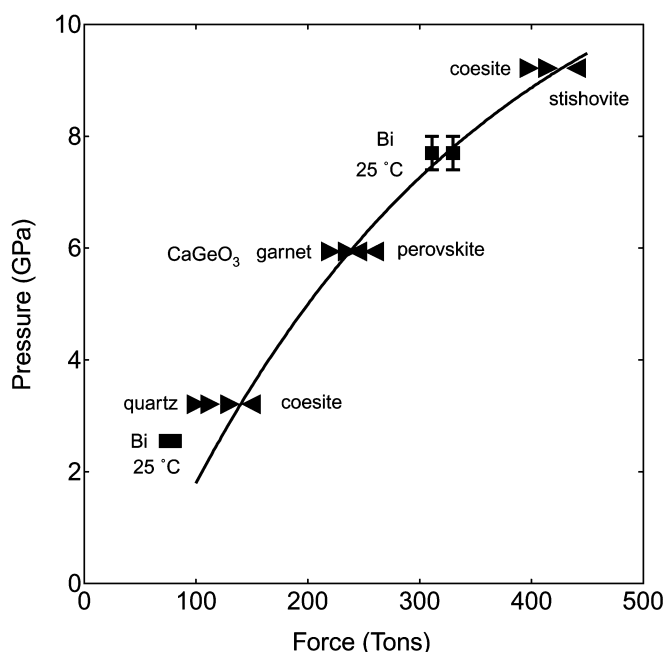


**Fig. 1** Pressure calibration curve for 12-mm truncated edge length anvils and castable octahedra, using the Walker style multi anvil at the University of Michigan. The curve is bracketed by 1,200 °C experiments. *Solid squares* 25 °C calibrations; *solid triangles* 1,200 °C calibrations

No correction was made for the effect of pressure on thermocouple EMF. Experiments were cooled by turning off the power to the heater, and pressure was released at a rate slower than  $1 \text{ GPa h}^{-1}$ . Following recovery, the capsule was pierced and the presence or absence of water recorded. Sample material was extracted from the end of the capsule that was in contact with the thermocouple; the total volume of material selected for analysis was located within about 0.5 mm of the thermocouple junction. In experiments close to the  $\text{CaGeO}_3$  garnet–perovskite and  $\text{SiO}_2$  coesite–stishovite phase boundaries, the thermocouple junction was packed with  $\text{CaGeO}_3$  or  $\text{SiO}_2$  as an in situ pressure marker. Recovery and analysis of these internal calibrants provides an additional check of pressure with respect to the calibration reactions.

## Analyses

The run product rutile is colorless and has crystal sizes in the range of 1–10  $\mu\text{m}$ . The  $\text{TiO}_2\text{II}$  has crystal sizes of up to 30  $\mu\text{m}$ , and appears to be nearly opaque due to internal reflections unless thin edges are examined, and there it is also colorless. The refractive index and birefringence of  $\text{TiO}_2\text{II}$  are too high to measure with oil-immersion techniques. The reflectivity of both polymorphs is high, showing a light yellow color with reflected white light. Examination of polished epoxy mounts of both phases using back-scattered electron (BSE) imaging with the SEM reveals subhedral to euhedral crystals. The  $\text{TiO}_2\text{II}$  shows light red–orange cathodoluminescence (CL) with the electron microprobe, whereas the synthetic rutile and the synthetic  $\text{TiO}_2$  standard show no CL.

X-ray diffraction spectra of starting materials and experimental products were measured using a Scintag powder diffractometer with Cu K- $\alpha$  radiation. The diffraction spectra of synthesis products and starting mix were recorded over a range from 5 to  $85^\circ 2\theta$ . All of the peaks present match those of  $\text{TiO}_2$  phases. Material extracted from phase equilibrium experiments was analyzed between 25 and  $60^\circ 2\theta$  to determine the direction of reaction. In order to evaluate whether reaction took place during the experiment, we first calculate a hypothetical “extent of reaction,” assuming a linear relationship between relative peak heights of the principal  $\text{TiO}_2\text{II}$  (111,  $31.4^\circ 2\theta$ ) and rutile (110,  $27.4^\circ 2\theta$ ) reflections and their phase proportions. Because coarsening and reorientation may affect peak heights, such an estimate is not necessarily accurate. For example, in experiments at 500 and 600  $^\circ\text{C}$  the hypothetical “extent of reaction” does not correlate with experimental duration or pressure, suggesting that other factors (such as coarsening and reorientation) contribute to the peak intensity changes. Furthermore, we observe differences in the relative heights of 110 and 211 peaks in rutile in the starting material, and in rutile recrystallized in these experiments. Likewise, the 111 and 110 peaks in  $\text{TiO}_2\text{II}$

differ in relative intensity in the starting material and in experimental products. Unfortunately, the quality of the diffraction spectra of our small experimental samples is inadequate for further quantification of this effect. Hence, we adopt the arbitrary criterion that a phase change is deemed to have occurred during an experiment only when the estimated extent of reaction is greater than 30%.

Because water was present in most experiments to shorten the time to reach equilibrium, it is necessary to show that water does not affect the phase equilibrium, i.e., water does not enter either phase in significant proportion. It is conceivable that water could be introduced into the structure of either polymorph, e.g., by reduction of  $\text{Ti}^{4+}$  to  $\text{Ti}^{3+}$ , forming  $\text{TiOOH}$ , or due to the presence of impurities such as  $\text{Cr}^{3+}$  forming  $\text{CrOOH}$ . To verify the absence of a significant hydrous component in  $\text{TiO}_2$  phases, crystals of rutile and  $\text{TiO}_2\text{II}$  were analyzed using infrared spectroscopy. The crystals were taken out of the experimental capsules (experiments RUT #12 and RUT #13) and placed on a  $\text{BaF}_2$  window under an IR microscope. The microscope aperture was  $10 \times 10 \mu\text{m}$  square. The largest rutile crystals are about 5  $\mu\text{m}$  across; hence, IR spectra were obtained either on an aggregate of crystals, or on a region that includes both rutile and empty space. The largest  $\text{TiO}_2\text{II}$  crystals are about 20  $\mu\text{m}$  across, so single crystals were analyzed. No attempt was made to orient, polish, or identify individual crystals. Rutile from experiment RUT #12 and  $\text{TiO}_2\text{II}$  from experiment RUT #13 were examined in the near-infrared (NIR), and spectra ( $2,000\text{--}9,000 \text{ cm}^{-1}$ ) show no detectable hydrous band for both rutile and  $\text{TiO}_2\text{II}$  phases. Applying the molar absorption coefficient for rutile (Maldener et al. 2001) to both phases, and assuming thicknesses of 5  $\mu\text{m}$  for rutile and 20  $\mu\text{m}$  for  $\text{TiO}_2\text{II}$ , the  $\text{H}_2\text{O}$  content of rutile is estimated to be  $< 400 \text{ ppm H}_2\text{O}$ , while that of  $\text{TiO}_2\text{II}$  is estimated to be  $< 100 \text{ ppm}$ .

Samples of rutile and  $\text{TiO}_2\text{II}$  were analyzed for titanium and oxygen using a CAMECA MBX electron microprobe and synthetic  $\text{TiO}_2$  as a standard. A long-duration EDS scan showed no other peaks. Quantitative analyses were conducted at 15 kV, 20 nA, 60 s count times and a point beam. Wavelength scans of the oxygen K $\alpha$  peak showed no interference with the Ti L $\beta$  peak with an OV60 spectrometer crystal. There is an interference between a minor Ti peak (Ti L $\beta_{3,4}$ ) and the O K $\alpha$  peak identified by scanning Ti metal that is not resolved. However, the use of  $\text{TiO}_2$  standard to analyze other  $\text{TiO}_2$  phases means that the 2% contribution to the oxygen from Ti L $\beta_{3,4}$  is identical for both standard and unknown and, therefore, does not perturb the analysis. A wavelength scan on O K $\alpha$  was used to select backgrounds at  $\pm 3,500 \sin\theta$  steps shifted from the peak position. Analytical totals were 99.84–99.94 wt%. The average atomic composition for rutile is  $0.334 \pm 0.001$  for Ti and  $0.666 \pm 0.003$  for O (experiment RUT #12). The average atomic composition for  $\text{TiO}_2\text{II}$  is  $0.335 \pm 0.001$  for Ti and  $0.665 \pm 0.003$  for O (experiment

RUT #13). Hence, within analytical error, the TiO<sub>2</sub> phases are stoichiometric with insignificant OH and other components.

## Results

The result of synthesis and phase equilibrium experiments is given in Table 1 and shown in Fig. 2. The phase boundary has been bracketed by hydrothermal experiments at 700, 1,000, and 1,200 °C, in which reaction has proceeded nearly to completion, and is described by the equation:

$$P(\text{GPa}) = 1.29 + 0.0065T(^{\circ}\text{C}) \quad (1)$$

Although growth of TiO<sub>2</sub>II was measured in experiments at 500 and 600 °C, reaction rates were sluggish, and we have not succeeded in growing rutile at these temperatures. The error bars in Fig. 2 represent an estimate of the uncertainty in pressure, derived from the width of the reaction brackets in the pressure calibration and the slope of the calibration curve at that point (Fig. 1). This results in a larger uncertainty at the lower end of the pressure range, and does not include any effect of temperature on the calibration. We observe a significant decrease in efficiency (pressure/force) with increasing temperature from 25 to 1,200 °C, which is consistent with previous observations (e.g., Fei and Bertka 1999). Thus, it is possible that our lowest temperature experiments may require an additional pressure correction, meaning that the pressure was actually higher than reported in Table 1 and Fig. 2. In experiments at 700 °C, however, the CaGeO<sub>3</sub> internal pressure marker was recovered as garnet, indicating that no upward revision of pressure is required at that temperature. The SiO<sub>2</sub> phases recovered from experiments at 1,200 °C are also consistent with the reported pressures. Anhydrous synthesis experiments at 1,200 °C are consistent with the phase boundary determined in the fluid-bearing experiments, which further suggests that the equilibrium is unaffected

by the presence of water. Infrared spectra of TiO<sub>2</sub>II from experiments RUT #2 and RUT #13 did not contain bands related to hydrous species, from which we conclude that TiO<sub>2</sub>II is not stabilized by the presence of water.

## Discussion

The curved phase boundary of Olsen et al. (1999) is attributable to kinetic effects. Growth of the high-pressure

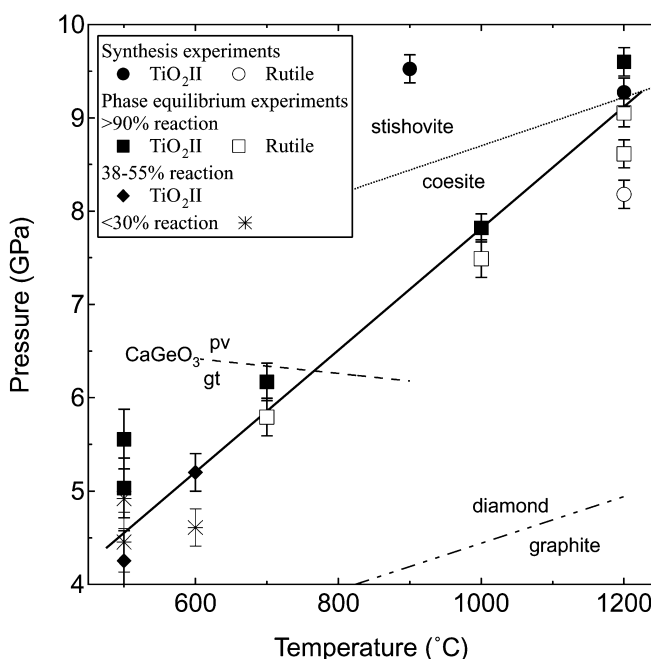


**Fig. 2** Results of hydrothermal phase equilibrium experiments and nominally dry synthesis experiments. Growth of rutile is indicated by *open circles*, and the *closed symbols* signify growth of TiO<sub>2</sub>II. The phase boundary between rutile and TiO<sub>2</sub>II, based on the results of the phase equilibrium experiments, is shown as a *solid line*. *Broken lines* represent the phase boundaries between CaGeO<sub>3</sub> garnet/perovskite (Susaki et al. 1985), coesite/stishovite (Zhang et al. 1993) and graphite/diamond (Kennedy and Kennedy 1976)

**Table 1** Results of phase equilibrium experiments

Experiment	P (GPa)	T (°C)	Duration (h)	Starting material	TiO <sub>2</sub> II growth <sup>a</sup> (%)
RUT #7	3.9	500	41.1	Ru50–TiO <sub>2</sub> II50	–10
RUT #6	4.3	500	19.6	Ru50–TiO <sub>2</sub> II50	38
RUT #4	4.5	500	17.0	Ru50–TiO <sub>2</sub> II50	24 <sup>b</sup>
RUT #3	4.9	500	14.8	Ru50–TiO <sub>2</sub> II50	27 <sup>b</sup>
RUT #2	5.0	500	14.5	Ru50–TiO <sub>2</sub> II50	94
RUT #1	5.6	500	24.0	Ru50–TiO <sub>2</sub> II50	97
RUT #18	4.6	600	237.9	Ru50–TiO <sub>2</sub> II50	21
RUT #17	5.2	600	32.9	Ru50–TiO <sub>2</sub> II50	55
RUT #12	5.8	700	16.9	Ru50–TiO <sub>2</sub> II50	–100
RUT #13	6.2	700	21.1	Ru50–TiO <sub>2</sub> II50	98
RUT #19	7.5	1,000	1.9	Ru50–TiO <sub>2</sub> II50	–100
RUT #15	7.8	1,000	3.1	Ru50–TiO <sub>2</sub> II50	94
RUT #14	8.6	1,200	2.0	Ru50–TiO <sub>2</sub> II50	–100
RUT #16	9.1	1,200	1.0	Ru50–TiO <sub>2</sub> II50	–100
RUT #20	9.6	1,200	1.2	Rutile	95
RUT #5	8.2	1,200	1.7	Anatase	–100 <sup>c</sup>
RUT #8	9.3	1,200	2.0	Anatase	97 <sup>c</sup>

<sup>a</sup>Positive numbers indicate growth of TiO<sub>2</sub>II and negative numbers indicate rutile growth

<sup>b</sup>Water escaped during experiment

<sup>c</sup>Anhydrous synthesis

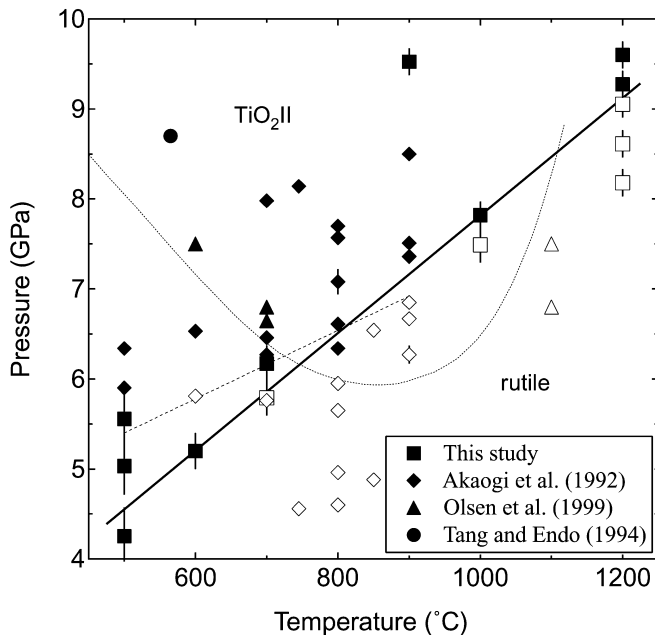


**Fig. 3** Comparison with previous results. Data from this study (square symbols) and inferred phase boundary (solid line) are compared with data from Akaogi et al. (1992; diamonds and dashed line), Tang and Endo (1994; circle) and Olsen et al. (1999; triangles and dotted curve). Data from the latter study are only included where growth of a phase has been observed. Data from this study are only included where  $> 30\%$  reaction has occurred. In all cases, filled and open symbols represent, respectively,  $\text{TiO}_2\text{II}$  and rutile stability

phase in experiments at 5.0–5.6 GPa and 500 °C shows that  $\text{TiO}_2\text{II}$  is not restricted to pressures greater than 6 GPa, as concluded by Olsen et al. (1999). The lack of high-pressure phase growth at low temperatures is best explained by sluggishness of the phase transition. For instance, a careful kinetic study of the coesite-stishovite transition by Zhang et al. (1996) produced a curved boundary for the first appearance of stishovite that is strikingly similar to that of Olsen et al. (1999), even though the equilibrium transition is nearly linear (Fig. 2). Taking into account the kinetic effect (i.e., disregarding data at low temperatures), the results of Olsen et al. (1999) are in accord with our proposed phase relations.

The phase relations determined in this study are broadly in accord with Akaogi et al. (1992; Fig. 3). Our reversal experiments were at 700, 1,000, and 1,200 °C, whereas the in situ experiments of Akaogi et al. (1992) covered 600–900 °C. Our bracket at 700 °C is in perfect agreement with the reversals of Akaogi et al. (1992) at the same conditions. At temperatures of 500 to 600 °C, the “extent of reaction” in most of our experiments (durations of 14 to 238 h) is not sufficiently high to rule out the effect of coarsening and reorientation on the x-ray peak intensity. On the other hand, Akaogi et al. (1992) constrained the 600 °C phase boundary using 10–20-min experiments. It is not clear what caused the difference in the required duration to reach equilibrium.

Experiments at 500 and 600 °C, in which the direction of reaction can be inferred without ambiguity, are consistent with the phase boundary, as constrained by the higher temperature experimental brackets.

The phase boundary determined in this study has a somewhat steeper slope ( $dP/dT$ ) than that of Akaogi et al. (1992; solid and dashed lines in Fig. 3), but is still consistent with all but two of their data points. At 600 °C and 5.2 GPa we observe growth of  $\text{TiO}_2\text{II}$ , which we find hard to reconcile with their observation of rutile growth at 600 °C and 5.8 GPa. The observation of  $\text{TiO}_2\text{II}$  growth at 800 °C and 6.34 GPa by Akaogi et al. (1992) is inconsistent with both their own proposed boundary and our proposed boundary. Notwithstanding the discrepancy at low temperature, the phase boundary is well constrained by our reversals at 700, 1,000, and 1,200 °C, as well as the reversals of Akaogi et al. (1992) at 700 and 900 °C. While we cannot claim the same precision in pressure determination as is possible in an in situ study, we are able to conduct long duration experiments (up to 10 days) over a larger pressure and temperature range. These advantages, together with our use of pressure markers, give us confidence in the phase relations shown in Eq. (1), and Figs. 2 and 3. In addition, after accounting for kinetic effects, observation of phase growth from the in situ studies of Olsen et al. (1999) and Tang and Endo (1994) is consistent with our proposed phase relations.

Hwang et al. (2000) discovered an epitaxial, nanometer-thick slab of  $\text{TiO}_2\text{II}$  sandwiched between twinned rutile included in a garnet crystal in diamondiferous gneiss from Germany. They used the U-shaped rutile- $\text{TiO}_2\text{II}$  nanophase boundary of Olsen et al. (1999) and inferred that the host rock experienced a minimum pressure of 4 to 5 GPa. In the light of our clarification of the  $\text{TiO}_2$  phase diagram, the implication of the  $\text{TiO}_2\text{II}$  lamella described by Hwang et al. (2000) should be reassessed. At 900–1,000 °C, pressures in excess of 7 GPa would be required to stabilize  $\text{TiO}_2\text{II}$  as a bulk phase. However, because the width of the  $\text{TiO}_2\text{II}$  lamella is only about 5 nm, bulk phase relations might not be applicable. Currently, there is no applicable phase diagram for the epitaxial nanophase system. The nanophase experiments of Olsen et al. (1999) were conducted on ultra fine-grained rutile that reacted to form presumably coarsened  $\text{TiO}_2\text{II}$ , rather than involving nanosize  $\text{TiO}_2\text{II}$  and coarse rutile. Furthermore, when rutile is included in garnet, the pressure in the rutile inclusion may differ from that on the garnet host (Rosenfeld and Chase 1961; Zhang 1998). Ignoring elastic anisotropy, calculations show that, however, the pressure difference between the inclusion and the host is not large. For example, if rutile were included in garnet in the first stage at 700 °C and 2 GPa, then at 900 °C and a host pressure of 6.6 GPa, the inclusion pressure would be 7.0 GPa. From the above consideration, it is likely that garnet with  $\text{TiO}_2\text{II}$ -bearing inclusions reflects a deeper origin than hitherto thought. Quantification of the pressure requires an understanding of the surface energies of rutile and  $\text{TiO}_2\text{II}$ .

## Conclusions

We have constrained the equilibrium phase boundary between rutile and TiO<sub>2</sub>II at 500–1,200 °C and 4.2–9.6 GPa. Within error the phase boundary is linear, in close agreement with the experiments of Akaogi et al. (1992), but in striking contrast to the phase diagram of Olsen et al. (1999). The new phase boundary is described by the equation:  $P \text{ (GPa)} = 1.29 + 0.0065 T \text{ (}^\circ\text{C)}$ . Growth of TiO<sub>2</sub>II in our experiments at 5.0–5.6 GPa and 500 °C shows that it is not restricted to pressures greater than 6 GPa, as was inferred by Olsen et al. (1999). Their results can be explained in terms of kinetics of the phase transition. After accounting for the kinetic effects, their observations of phase growth are in accord with our proposed phase relations. The thermobarometric implication of TiO<sub>2</sub>II in garnet (Hwang et al. 2000) also needs to be re-evaluated. At temperatures greater than 1,000 °C, TiO<sub>2</sub>II requires pressures more than 3 GPa in excess of the graphite–diamond transition.

**Acknowledgments** We are grateful to David Walker and Mark Schmitz for reviews. This research was supported by NSF grants EAR 01-06718, EAR 01-25506, and a University of Michigan grant. The electron microprobes at the University of Michigan were purchased with support by NSF grants EAR 82-12764 and 99-11352, the Hitachi SEM by EAR 96-28196, the powder X-ray diffractometer by EAR 95-08180, and the FTIR by EAR 99-72937.

## References

- Akaogi M, Kusaba K, Susaki J-I, Yagi T, Matsui M, Kikegawa T, Yusa H, Ito E (1992) High-pressure high-temperature stability of  $\alpha$ -PbO<sub>2</sub>-type TiO<sub>2</sub> and MgSiO<sub>3</sub> majorite: calorimetric and in situ X-ray diffraction studies. In: Syono Y, Manghnani MH (eds) High-pressure research: application to Earth and planetary sciences. TERRAPUB American Geophysical Union, Washington, DC, pp 447–455
- Bendeliany NA, Popova SV, Vereschagin LF (1966) A new modification of titanium dioxide stable at high pressure. *Geokhimiya* 1966:499–502
- Bose K, Ganguly J (1995) Quartz-coesite transition revisited—reversed experimental—determination at 500–1200 °C and retrieved thermochemical properties. *Am Mineral* 80:231–238
- Dachille F, Simons PY, Roy R (1968) Pressure-temperature studies of anatase, brookite, rutile and TiO<sub>2</sub>-II. *Am Mineral* 53:1929–1939
- Dubrovinsky LS, Dubrovinskaia NA, Swamy V, Muscat J, Harrison NM, Ahuja R, Holm B, Johansson B (2001) Materials science: the hardest known oxide. *Nature* 410:653–654
- El Goresy A, Chen M, Dubrovinsky L, Gillet P, Graup G (2001a) An ultradense polymorph of rutile with seven-coordinated titanium from the Ries Crater. *Science* 293:1467–1470
- El Goresy A, Chen M, Gillet P, Dubrovinsky L, Graup G, Ahuja R (2001b) A natural shock-induced dense polymorph of rutile with  $\alpha$ -PbO<sub>2</sub> structure in the suevite from the Ries crater in Germany. *Earth Planet Sci Lett* 192:485–495
- Fei Y, Bertka CM (1999) Phase transitions in the Earth's mantle and mantle mineralogy. In: Fei Y, Bertka CM, Mysen BO (eds) Mantle petrology: field observations and high-pressure experimentation: a tribute to Francis R. (Joe) Boyd, special publication no 6. Geochemical Society, Houston, pp 189–207
- Hayob JL, Bohlen SR, Essene EJ (1993) Experimental investigation and application of the reaction rutile + pyroxene = quartz + ilmenite. *Contrib Mineral Petrol* 115:18–37
- Hwang SL, Shen PY, Chu HT, Yui TF (2000) Nanometer-size  $\alpha$ -PbO<sub>2</sub>-type TiO<sub>2</sub> in garnet: a thermobarometer for ultrahigh-pressure metamorphism. *Science* 288:321–324
- Jamieson JC, Olinger B (1969) Pressure-temperature studies of anatase, brookite, rutile and TiO<sub>2</sub>(II): a discussion. *Am Mineral* 54:1477–1481
- Kennedy CS, Kennedy GC (1976) The equilibrium boundary between graphite and diamond. *J Geophys Res* 81:2467–2470
- Maldener J, Rauch F, Gavranic M, Beran A (2001) OH absorption coefficients of rutile and cassiterite deduced from nuclear reaction analysis and FTIR spectroscopy. *Min Petrol* 71:21–29
- Olsen JS, Gerward L, Jiang JZ (1999) On the rutile/ $\alpha$ -PbO<sub>2</sub>-type phase boundary of TiO<sub>2</sub>. *J Phys Chem Solids* 60:229–233
- Piermarini GJ, Block S (1975) Ultrahigh pressure diamond-anvil cell and several semiconductor phase transition pressures in relation to fixed point pressure scale. *Rev Sci Instr* 46:973–979
- Rosenfeld JL, Chase AB (1961) Pressure and temperature of crystallization from elastic effects around solid inclusions in minerals? *Am J Sci* 259:519–541
- Sato H, Endo S, Sugiyama M, Kikegawa T, Shimomura O, Kusaba K (1991) Baddeleyite-type high-pressure phase of TiO<sub>2</sub>. *Science* 251:786–788
- Shen PY, Hwang SL, Chu HT, Yui TF (2001)  $\alpha$ -PbO<sub>2</sub>-type TiO<sub>2</sub>: from mineral physics to natural occurrence. *Int Geol Rev* 43:366–378
- Susaki J, Akaogi M, Akimoto S, Shimomura O (1985) Garnet–perovskite transformation in CaGeO<sub>3</sub>: in situ X-ray measurements using synchrotron radiation. *Geophys Res Lett* 12:729–732
- Tang J, Endo S (1994) X-ray study of the transitions among the rutile,  $\alpha$ -PbO<sub>2</sub> and baddeleyite phases of TiO<sub>2</sub> at high pressure and high temperature. In: Schmidt SC, Shaner JW, Samara GA, Ross M (eds) High-pressure science and technology. American Institute of Physics, pp 367–370
- Walker D, Carpenter MA, Hitch CM (1990) Some simplifications to multianvil devices for high-pressure experiments. *Am Mineral* 75:1020–1028
- Zhang JZ, Liebermann RC, Gasparik T, Herzberg CT, Fei YW (1993) Melting and subsolidus relations of SiO<sub>2</sub> at 9–14 GPa. *J Geophys Res* 98:19785–19793
- Zhang J, Li B, Utsumi W, Liebermann RC (1996) In situ X-ray observations of the coesite-stishovite transition: reversed phase boundary and kinetics. *Phys Chem Mineral* 23:1–10
- Zhang Y (1998) Mechanical and phase equilibria in inclusion-host systems. *Earth Planet Sci Lett* 157:209–222